FEATURE ARTICLE

ChemComm www.rsc.org/chemcomm

Iron oxide chemistry. From molecular clusters to extended solid networks

Jean-Pierre Jolivet, Corinne Chanéac and Elisabeth Tronc

Chimie de la Matière Condensée, UMR-CNRS 7574, Université P&M Curie, 4 place Jussieu, 75252 Paris, France. E-mail: jpj@ccr.jussieu.fr

Received (in Cambridge, UK) 24th April 2003, Accepted 25th September 2003
First published as an Advance Article on the web 23rd January 2004

This overview features the chemical background on condensation phenomena of iron cations in aqueous solution. The formation of molecular clusters or nanosized solid phases is interpreted with illustrative mechanisms building a bridge between solution chemistry and solid state chemistry. Iron chemistry gives a very nice example of chemical versatility.

1 Introduction. The importance of iron in various fields, from nanoparticles for magnetic recording to natural systems

The chemistry of iron is of great interest because iron is an abundant element present in various fields. Metallurgy has been developed relating to iron and iron oxides are used for various applications, colored pigments, magnetic materials, catalysts…[1] Ferro- and ferrimagnetic materials have been receiving growing interest for both technological and theoretical reasons, especially in the context of magnetic recording. The properties of finely divided magnetic materials closely depend on the size of the particles and their state of dispersion and aggregation.[2] It is therefore very important to carefully control the synthesis of particles and their surface state. Iron is also an important element in the environment, because of its presence in the chemistry of soils and natural waters under the form of molecular complexes or colloids. Dissolution of ferric oxides in natural conditions (including acid-base and redox phenomena, microbial mediation and photochemistry) is of major importance in the cycling of iron.[3] Iron oxides are also present in living organisms (*e.g.* plants, bacteria, molluscs, birds and humans). Fe(II) complexes are the active center of haemoglobin and ferredoxins, and various biomineralization processes involve Fe(II) and Fe (III) species for the regulation of iron concentration in organism (ferritin) or, in various occurrences, to produce different oxides, such as goethite, magnetite, lepidocrocite.[4]

The structural chemistry of iron oxy(hydroxi)des is very rich and diversified. More than a dozen structural types exist for ferrous, ferric and mixed valent compounds.[5] Almost all of them can be formed from solutions by "chimie douce" giving rise to a puzzling chemistry.[1,6,7] The high versatility of iron chemistry in aqueous medium comes from the occurrence of two stable oxidation states on a large range of acidity, and from the high reactivity of iron complexes towards acid–base phenomena. Because of the great diversity of physico-chemical conditions in the environment (acidity, redox conditions, bacterial activity, temperature, salinity, presence of organic or inorganic ligands…), it is not surprising to find practically all the iron oxide phases in the conditions of natural environment.

The aim of this article is to present the main aspects of iron chemistry in aqueous medium, especially the condensation phenomena which lead to the formation of clusters or particles. We present the main factors – in the laboratory – allowing us to orient the crystallization process of solids and to control the particle size. We also examine some aspects of the synthesis of magnetic phases and nanomaterials.

2 The Fe^{2+} and Fe^{3+} cations in aqueous solution: acidity, hydroxylation and limited condensation. Molecular clusters

Like many elements in water, the iron cations form hexacoordinated aquo complexes, $[Fe(OH_2)_6]^{z+}$ in which the polarization of coordinated water molecules is strongly dependent on the formal charge (oxidation state) and size of the cation. This makes the ferric aquo complexes more acidic than ferrous complexes and hydroxylation of the cations occurs on very distinct ranges of pH, as indicated by speciation diagrams[8] (Fig. 1).

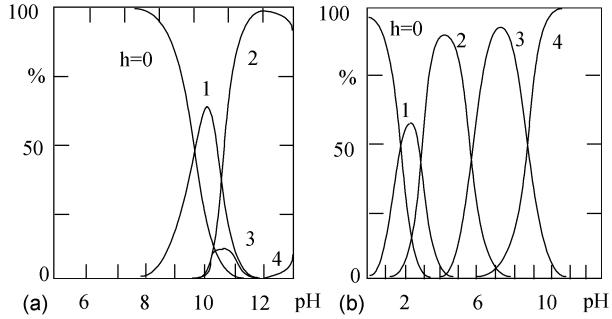

Fig. 1 Speciation of $[Fe(OH)_h(OH_2)_{6-h}]^{(z-h)+}$ complexes of (a) Fe(II) ; (b) Fe(III). Adapted from (8).

Hydroxylated complexes condense *via* two basic mechanisms, depending on the nature of the coordination sphere of the cations.[7] Condensation of aquohydroxo complexes proceeds by olation with elimination of water and formation of hydroxo bridges:

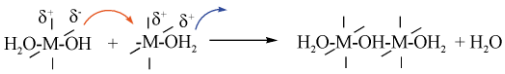

For oxohydroxo complexes, there is no water molecule in the coordination sphere of the complexes and therefore no leaving group. Condensation has to proceed in this case *via* a two-step associative mechanism leading to the formation of oxo bridges (oxolation):

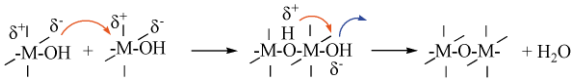

For iron complexes, condensation occurs from strongly acidic media (pH $\geq$ 1) for ferric species while ferrous complexes condense only above pH 6.[7] In fact, the formation of ferrous polycationic species is poorly documented. As for many divalent elements in solution,[7] a compact tetrameric polycation $[Fe_4(OH)_4(OH_2)_{12}]^{4+}$ may form (Fig. 2) at the first stage of hydroxylation ($[Fe(OH)_h(OH_2)_{6-h}]^{(2-h)+}$ with $h = 1$) but, to our knowledge, no evidence has so far been reported.

The chemistry of ferric species is extremely complicated, in comparison to that of other trivalent elements (Al, Cr). Due to their high reactivity, ferric complexes condense very rapidly and it is difficult to stop the process at molecular level, *i.e.* polycationic

DOI: 10.1039/b304532n

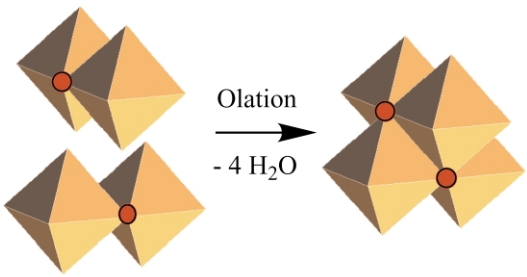

Fig. 2 Formation of the $[Fe_4(OH)_4(OH_2)_{12}]^{4+}$ polycation from dimers $[Fe_2(OH)_2(OH_2)_8]^{2+}$.

species. The control of the reactivity requires the use of very strong complexing polydentate ligands. Many polycationic ferric species have nicely been obtained for instance with various polycarboxylate or amino ligands.[9] (Fig. 3) It is interesting to note that,

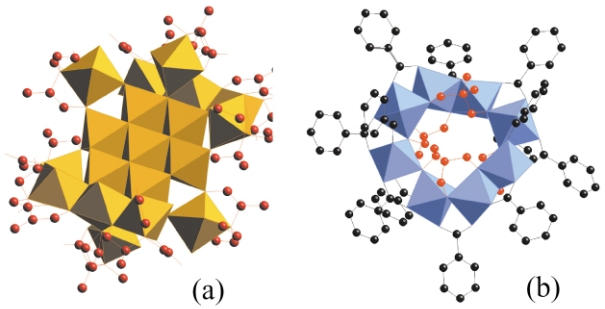

Fig. 3 Examples of polycationic structures formed by ferric ions in the presence of strongly complexing ligands: (a) $[Fe_{19}O_6(OH)_{14}(L)_{10}(H_2O)_{12}]^+$ L = $N(CH_2COOH)_2(CH_2CH_2OH)$ and (b) $Fe_8(PhCOO)_{12}(thme)_4{\cdot}2Et_2O$ (thme: trishydroxymethylethane).

at variance with chromium (III)[10] and aluminium polycations, ferric ions are more often bounded by oxo than hydroxo brigdes. This seems to result from the higher electronegativity of iron than of chromium and aluminium.

3 Why and how do the solid phases form?

In the absence of strongly complexing ligands, the control of the acidity enables the formation of the aquo hydroxo zero-charge complex, which is the precursor of the solid.[7] The crystal chemistry of the two cations Fe^{2+} and Fe^{3+} is also extremely different.

3.1 Ferrous compounds

Hydroxylation of ferrous ions at the stage $[Fe(OH)_2(OH_2)_4]^0$ occurs at pH > 6–7 and, under anaerobic conditions, leads to the precipitation of the hydroxide $Fe(OH)_2$. Like many hydroxides of divalent elements, $Fe(OH)_2$ has the brucite structure. It is easy to understand how (Fig. 4) this structural type is formed.[7] As there is no structural relationship between the compact tetramers (Fig. 2) and the hydroxide, the nuclei of the solid phase could be planar tetramers $[M_4(OH)_8(OH_2)_8]^0$ formed by olation between neutral species. Zero-charge dimers similar to those involved in the formation of compact tetramers can create μ_3–OH bridges as they are forming the planar tetramer, because of the bifunctionality of the precursor $[Fe(OH)_2(OH_2)_4]^0$. The growth of nuclei, always by olation, must take place rapidly in the plane, and so leads to the layered brucite-type structure.

This example shows very well that the polycations eventually formed during the hydroxylation process are not building blocks for the solid phase. The change in acidity of the medium leads to an important change in the structure of the polycations during the lowering of their charge. As a rule, there is no structural relationship between the solid and the polycations formed at lower hydroxylation stages. Chromium (III) is an exception because of its strong chemical inertness against substitution reactions.[11,7]

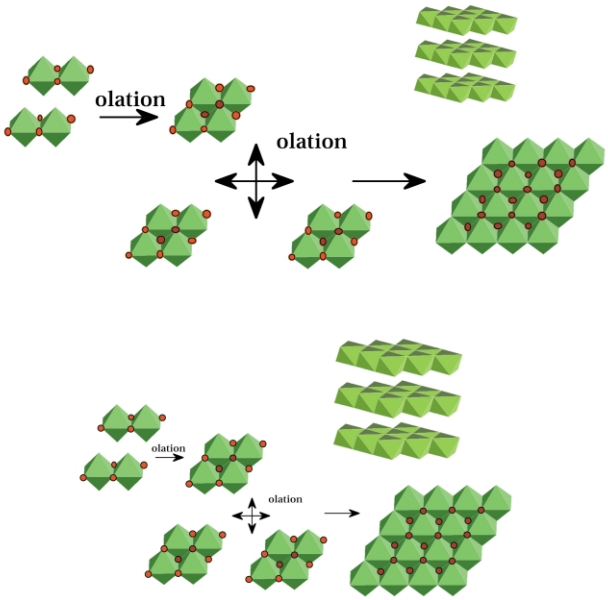

Fig. 4 A possible reaction pathway for the formation of $Fe(OH)_2$.

In solid state or aqueous suspension, the ferrous phases are very sensitive to oxidation. Various phases (green rusts, magnetite, goethite, lepidocrocite) can be formed, depending on the conditions (Section 3.3 Mixed ferric-ferrous compounds). It is to note that the unique way to form lepidocrocite, γ–FeOOH (Fig. 5), a ferric

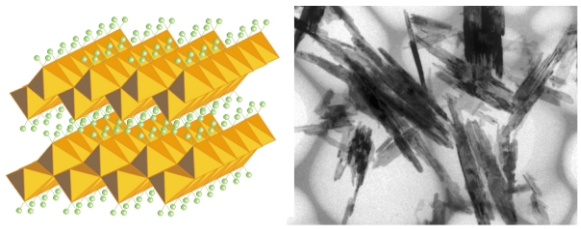

Fig. 5 Crystal structure of lepidocrocite γ–FeOOH and image of particles resulting from oxidation of $Fe(OH)_2$.

oxyhydroxide isostructural with boehmite γ–AlOOH, is the rapid oxidation of $Fe(OH)_2$ in suspension at pH around 7. In these conditions, oxidation occurs at the minimum of solubility of ferric complexes (see Section 3.2) ruling out a dissolution–crystallization process for the structural transformation. It presumably results from solid state reaction involving local rearrangements of chains of octahedra and forming the corrugated planes of the oxyhydroxide phase (Fig. 5). Such a transformation gives lath shaped particles of γ–FeOOH.

3.2 Ferric compounds. Influence of acidity, temperature and complexation in solution on the crystalline structure and particle size

Hydroxylation of ferric ions by addition of base in solution at room temperature (pH > 3) leads quasi instantaneously to a poorly defined highly hydrated phase, called 2-line ferrihydrite[12] because its X-ray diffraction pattern exhibits only two broad bands. Due to its poor structural organization, ferrihydrite is thermodynamically unstable. Its transformation proceeds *via* different pathways depending on the acidity of the medium and leads to different phases. At $5 \leq pH \leq 8$ (Fig. 6), ferrihydrite transforms into very small particles of haematite.[13] The solubility of the solid being very low (around 10^{-10} mol l^{-1}), the transformation can proceed only by dehydration *in situ* and local rearrangement. This explains the formation of an oxide and the very small size of crystalline domains.

When the solubility of ferrihydrite is higher (pH < 4 or pH > 8), the transformation can proceed more easily *via* a dissolution–

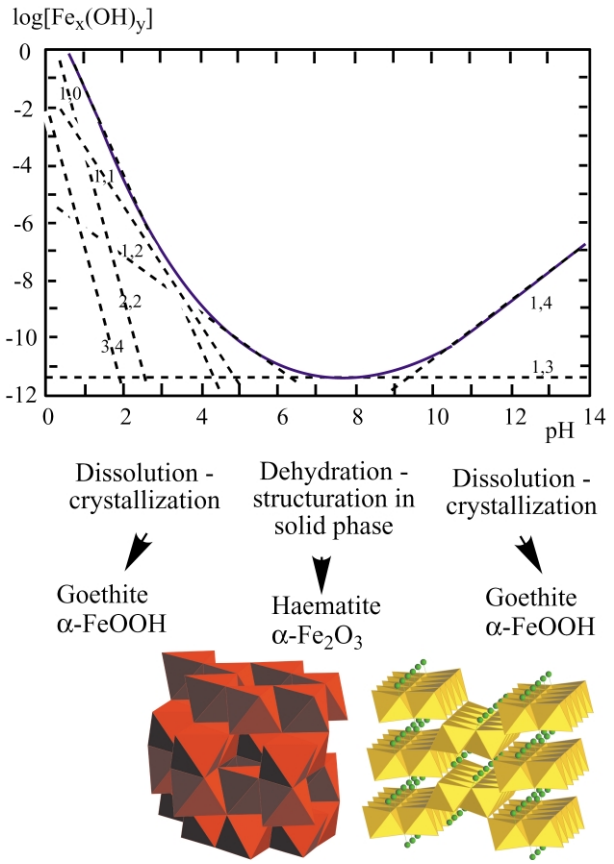

Fig. 6 Influence of pH on the solubility of iron and ferric (hydro)oxide crystal structures.

crystallization process, leading to goethite. (In contrast with aluminium, ferric hydroxide "Fe(OH)$_3$" does not exist and has never been identified; in similar pH conditions, aluminium forms the oxyhydroxide γ–AlOOH boehmite by *in situ* organization, and hydroxides Al(OH)$_3$ gibbsite or bayerite by dissolution crystallization.[14]) Complexing ligands such silicate[15] and especially phosphate,[16] delay or avoid the transformation of ferrihydrite into crystalline phases. This is for instance the case in very old soils in New Zealand (200 000 years!)[17] or in living organisms, in ferritin nanoparticles in which iron(III) is stocked.[4]

Growth of goethite by dissolution-crystallization process may be interpreted as taking place from the planar tetramer $[M_4(OH)_{12}(OH_2)_4]^0$. Condensation of these species by olation can lead directly to embryos of double chains of octahedra, characteristic of the structure of goethite. The chains connect by oxolation because of the relative kinetics of each reaction. Connection between the double chains occurs through μ_3–O bridges and hydrogen bonds between the chains (Fig. 7).

By controlling the acidity and ionic strength of the medium, we obtained very concentrated and stable dispersions of non aggregated particles. Such dispersions behave as nematic lyotropic liquid crystals exhibiting interesting magnetic properties.[18] The nematic phase aligns in a very low magnetic field (20 mT for samples 20 μm thick). The particles orient along the field direction at intensities smaller than 350 mT but reorient perpendicular to the field beyond 350 mT. This outstanding behavior could have interesting applications.

Thermolysis at 90–100 °C of acidic ferric solutions (pH ≤ 3) leads to haematite.[1,7] In these conditions, olation and oxolation compete and acidity facilitates oxolation leading to oxide. The acidity and the nature of the anions are however crucial for the control of the size of particles. At low concentration of chloride (C < 10^{-3} mol l^{-1}), 6-line ferrihydrite forms initially.[1,12] It

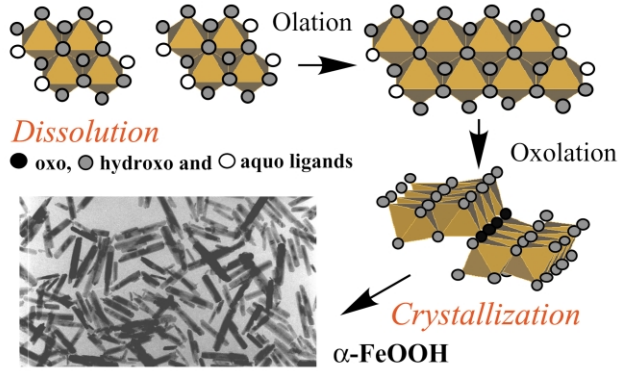

Fig. 7 A possible reaction pathway for the formation of goethite α–FeOOH in solution *via* ageing or thermolysis.

transforms into haematite during thermolysis but the particle size depends strongly on the acidity of the medium.[19] (Fig. 8). At high

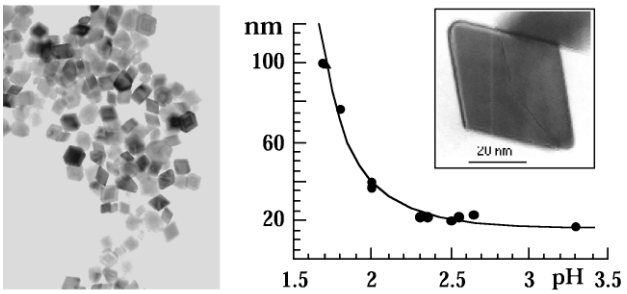

Fig. 8 Particles of haematite obtained by thermolysis at 95 °C of ferric nitrate solutions. Influence of the pH of the medium on the mean size of particles. From Ref. 19.

concentration of chloride, akaganeite, β–FeOOH, is first formed.[20] This metastable phase is slowly transformed into haematite during thermolysis and large (micronic) polycrystalline particles with various morphologies are obtained depending on the nature of anions in the medium.[21]

3.3 Mixed ferric-ferrous compounds: from green rusts to spinel

The presence of ferrous and ferric ions in solutions orients the condensation process to the formation of specific phases, namely the green rusts, of hydrotalcite structural type, and magnetite or maghemite, of spinel structural type. The formation of these mixed phases depends on many factors such as the iron concentration, pH and especially the system composition defined as $x = Fe^{3+}/(Fe^{2+} + Fe^{3+})$ (Fig. 9).

These phases are of high importance because green rusts are reactive intermediate products in aqueous corrosion of iron and are abundantly found in reductomorphic soils. Spinel oxides are ferrimagnetic materials usable for many technological applications.

3.3.1 Green rusts. For $x \leq 0.66$ and $HO^-/Fe_{total} = 2$ (pH ≈ 8), hydroxylation of the mixture forms a green rust (GR), a phase derived from brucite structure in which Fe^{2+} and Fe^{3+} ions fill the octahedral sites giving a positive charge to the sheets (Fig. 8). This positive charge is balanced by anion intercalation and there are in fact several structural families depending on the nature of the intercalated anions. The structural prototype is a carbonated phase, pyroaurite $[Mg_6Al_2(OH)_{16}]CO_3{\cdot}4H_2O$. With chloride or carbonate anions, green rust of type 1 with a variable Fe(II)–Fe(III) composition is formed while tetrahedral anions (sulfate, arsenate …) form green rust of type 2 with the unique composition Fe(II)/Fe(III) = 2.[22] The study of the progressive alkalization of Fe(II) and Fe(III) mixtures in the presence of sulfate ions, forming the phase

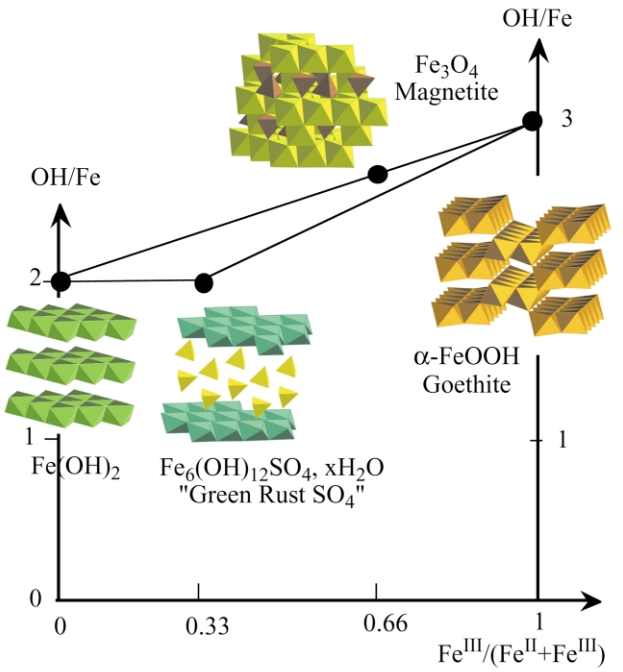

Fig. 9 Representation of the phases formed in solution as a function of the composition and hydroxylation ratio in the ferrous-ferric system.

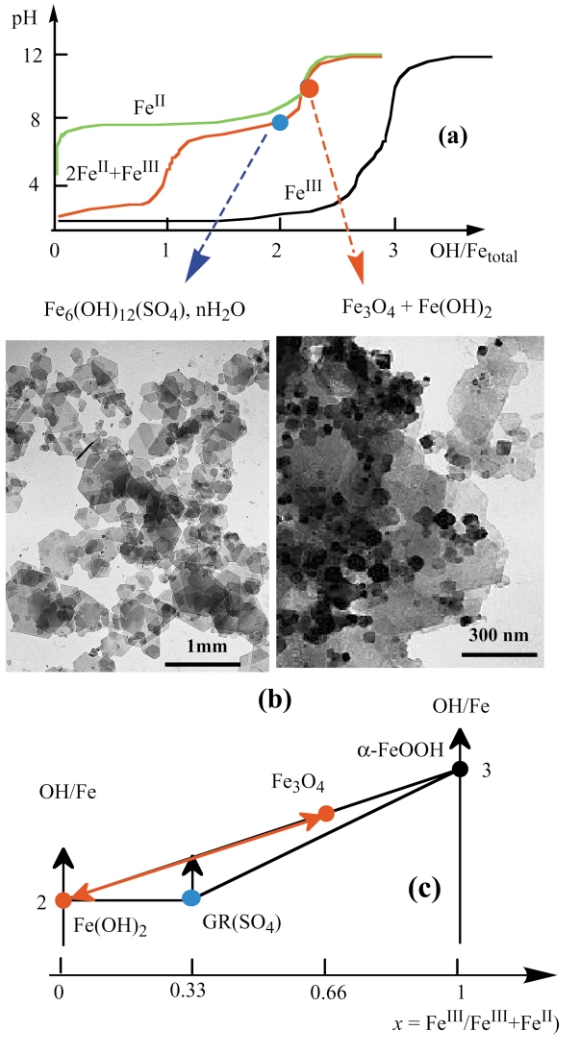

Fig. 10 pH titration curves of Fe(II), Fe(III) and a Fe(II)–Fe(III) mixture (x = 0.33) (a). Electron micrographs of products formed for OH/Fe_{total} = 2 and at the equivalent point (OH/Fe_{total} = 2.34) (b). Phase diagram showing the relation between GR, ferrous hydroxide and magnetite during alkalization. Adapted from (23).

$[Fe^{II}_4Fe^{III}_2(OH)_{12}]SO_4{\cdot}mH_2O$ for x = 0.33,[22] gives an interesting insight into the mechanism of formation. During the coprecipitation of ferric and ferrous ions, this phase forms following an heterogeneous crystallization process, because the two ions precipitate successively (Fig. 10).[23]

Up to pH 4, a purely ferric and poorly ordered hydroxysulfate forms on which, at higher pH, hydroxylated ferrous ions adsorb inducing the crystallization of GR phase. Crystallization proceeds according to dissolution-crystallization allowing the incorporation of sulfate anions into the structure. Surprisingly, the end of the formation of GR is not marked by an equivalent point in the pH-titration curve, and by raising pH up around 10, the equivalent point corresponds exactly to the transformation into magnetite and ferrous hydroxide (Fig. 10), as indicated by X-ray diffraction and Mössbauer spectroscopy.[23] This shows the metastability of GR against hydroxylation, according to the proposed phase diagram. It is interesting to note that GR phases can be formed following different pathways: oxidation of ferrous hydroxide, coprecipitation of ferric and ferrous ions, chemical, and electrochemical or biological reduction of lepidocrocite.[24] GRs appear as a turn-plate in many redox processes involving iron corrosion or transformation in natural environment.[25]

3.3.2 Magnetite. Magnetite Fe_3O_4 is easily obtained by coprecipitating aqueous Fe^{3+} and Fe^{2+} ions with x = 0.66. Iron ions are distributed into the octahedral (Oh) and tetrahedral (Td) sites of the fcc stacking of oxygen according to ($[Fe^{3+}]_{Td}[Fe^{3+}Fe^{2+}]_{Oh}O_4$). Magnetite is characterized by a fast electron hopping between the iron cations on the octahedral sublattice. Crystallization of spinel is quasi-immediate at room temperature and electron transfer between Fe^{2+} and Fe^{3+} ions plays a fundamental role in the process. In effect, maghemite, γ–Fe_2O_3, ($[Fe^{3+}]_{Td}[Fe^{3+}_{5/3}V_{1/3}]_{Oh}O_4$ where V stands for a cationic vacancy) does not form directly in solution by precipitation of ferric ions, but a small proportion of Fe^{2+} (≥ 10 mol %) induces the crystallization of all the iron into spinel. Studies[26,27] of the early precipitate revealed that all Fe^{2+} ions were incorporated into a Fe^{2+}-ferrihydrite forming a short-range ordered, mixed valence material exhibiting fast electron hopping, as evidenced by Mössbauer spectroscopy. Electron mobility brings about local structure rearrangements and drives spinel ordering. Besides this topotactic process, crystallization of spinel can also proceed by dissolution crystallization, resulting in two families of non-stoichiometric spinel particles ($[Fe^{III}]_{Td}[Fe^{III}_{1+2z/3}Fe^{II}_{1-z}V_{z/3}]_{Oh}O_4$) with very different mean size.[26] The relative importance of these two pathways depends on the Fe^{2+} level in the system and the end products of the coprecipitation are single phase only for $0.60 \leq x \leq 0.66$. The comparison with the cases where M^{2+} is different from Fe^{2+} emphasizes the role of electron mobility between Fe^{2+} and Fe^{3+} ions in the crystallization process. With other divalent cations, intervalence transfers are negligible and a spinel ferrite forms only by dissolution-crystallization.[28]

With x = 0.66, corresponding to stoichiometric magnetite, the mean particle size is monitored on the range 2–12 nm by the conditions of the medium, pH and ionic strength, I, imposed by a salt ($8.5 \leq pH \leq 12$ and $0.5 \leq I \leq 3$ mol.L^{-1}) (Fig. 11).[29]

Such an influence of acidity on the particle size is relevant to thermodynamics rather than kinetics (nucleation and growth processes). Acidity and ionic strength act on protonation–deprotonation equilibria of surface hydroxylated groups and, hence, on the electrostatic surface charge. This leads to a change in the chemical composition of the interface, inducing a decrease of the interfacial tension, γ, as stated by Gibbs's law, $d\gamma = -\Gamma_i d\mu_i$, where Γ_i is the density of adsorbed species i with chemical potential μ_i. Finally, the surface contribution, $dG = \gamma dA$ (A is the surface area of the system), to the free enthalpy of the formation of particles is lowered, allowing the increase in the system surface area.[14,29,30]

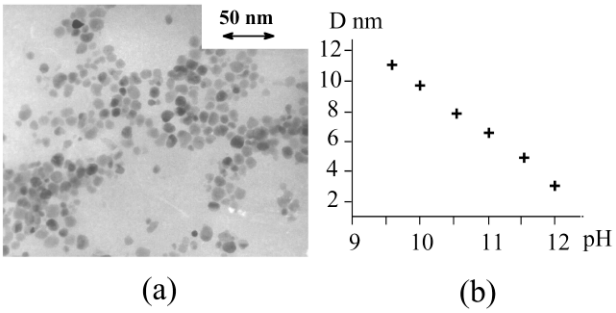

Fig. 11 (a) Micrograph of magnetite particles precipitated in aqueous medium. (b) Influence of the pH of precipitation on the mean particle size (ionic strength 3 mol l^{-1} imposed by $NaNO_3$).

3.4 Reactivity of spinel iron oxides: redox phenomena, formation of aqueous sols of maghemite

Due to the high electron mobility in the bulk, magnetite nanoparticles give rise to an interesting surface chemistry involving interfacial transfer of ions and/or electrons and allowing us to consider spinel iron oxide nanoparticles as refillable batteries.

Nanoparticles of magnetite are very sensitive to oxidation and transform into maghemite ($[Fe^{3+}]_{Td}[Fe^{3+}_{5/3}V_{1/3}]_{Oh}O_4$). The high reactivity is obviously due to the high surface-to-volume ratio and a controlled synthesis of particles requires strictly anaerobic conditions. However, aerial oxidation is not the only way to go to maghemite. Different interfacial ionic and/or electron transfers depending on the pH of the suspension can be involved in the transformation. In basic medium, the oxidation of magnetite proceeds by oxygen reduction at the surface of particles (electron transfer only) and coordination of oxide ions, while in acidic medium and anaerobic conditions, surface Fe^{2+} ions are desorbed as hexaaquo complexes in solution (electron and ion transfer) according to:[31]

$$[Fe^{3+}]_{Td}[Fe^{2.5+}_2]_{Oh}O_4 + 2\ H^+ \rightarrow 0.75\ [Fe^{3+}]_{Td}[Fe^{3+}_{5/3}V_{1/3}]_{Oh}O_4 + Fe^{2+} + H_2O$$

In both cases, the oxidation of Fe^{2+} ions is correlated with the migration of cations through the lattice framework, creating cationic vacancies in order to keep the charge balance (Fig. 12). The

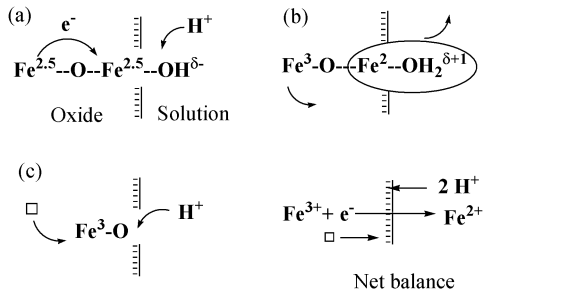

Fig. 12 Oxidation mechanism of magnetite to maghemite in acidic medium.

mobility of electrons on the octahedral sublattice renews the surface ferrous ions allowing the reaction to go to completion. The oxidation in acidic medium (pH ≈ 2) does not lead to noticeable size variation.

This reaction is apparently reversible. Adsorption of ferrous ions on maghemite particles by raising the pH proceeds so that the composition of magnetite (x = 0.66) is reached and all iron ions appear as "spinel iron" by Mössbauer spectroscopy. In fact, there is no migration of iron ions towards the interior of particles. Electrons (and presumably protons) are injected into the particle from the ferrous hydroxide adsorbed layer. This layer crystallizes as spinel and the reaction stops when equipopulation of $Fe^{3+}$and Fe^{2+} in the octahedral sublattice is reached.[32,33] Similar electron transfers occur during adsorption of ferric ions on magnetite,[34] or reduction of silver or platinum ions in suspension by magnetite, leading to a mixture of nanoparticles of maghemite and silver or platinum.[35]

Maghemite particles resulting from oxidation of magnetite can easily form very stable and concentrated aqueous dispersions. In acidic medium (pH 2) and at low ionic strength (10^{-2} — 5.10^{-2} mol.L^{-1}), maghemite nanoparticles carry a high positive charge density ($\sigma \approx 0.3$ C.m^{-2}), and so are well dispersable in water, forming cationic sols practically free from aggregation (Fig. 13, a, b).[36–38] The formation of such stable sols is a key step to the preparation of magnetic materials such as ferrofluids.[39]

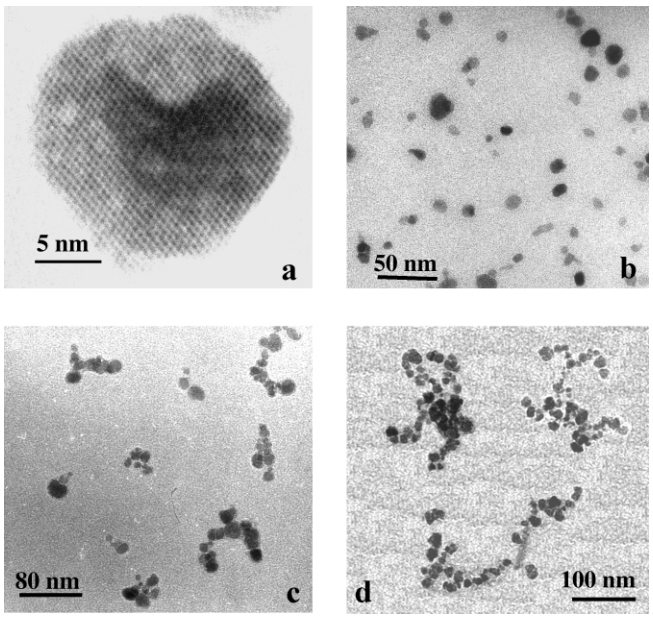

Fig. 13 Transmission electron micrographs of (a) a maghemite particle and (b, c, d) various states of dispersion in a polyvinylic alcohol.

3.5 Dispersion of maghemite particles in polymers and silica glasses: synthesis of nanocomposites

The dispersion of particles in organic[40] or inorganic[41] matrices, enabled the synthesis of various magnetic composite materials well-suited for studies on magnetism of nanoparticles, including measurements on unique particle.[42] Thermal treatment of silica-based composites led to the formation of a less common phase of iron oxide.

By adding a hydrosoluble polymer into the sol and drying the mixture, solid samples were obtained. This technique was used to prepare series of composites made up of maghemite particles with the same size distribution and different dispersion states in a polyvinylic alcohol, typically isolated particles with volumic concentration ranging from ~1% to 20% or aggregates of varying size and shape (Fig. 13), in order to study the magnetic properties of noninteracting particles and interparticle interaction effects.[2,43] Such materials enabled us to give the first experimental verification of the Néel–Brown model of the superparamagnetic relaxation for non-interacting particles.[44]

Composites made up of well dispersed maghemite particules in an epoxy resin were obtained by polymerization of the resin inside an organosol of particles.[45] The transfer of particles from aqueous medium to an organic solvent (sulfolane, propylene carbonate, hexamethylphosphorus-triamide) requires the adsorption of a coupling agent such as a phosphonic acid (phenylphosphonic acid, PPA). The head of the molecule, the phosphate group, strongly adsorbs onto particles as evidenced by infra-red and Mössbauer spectroscopies. The quadrupole doublet observed for the coated particles demonstrates the formation of a paramagnetic surface complex, due to the strong complexing ability of PPA for iron.[46] The hydrophobic tail (phenyl group) of the coupling agent allows

the dispersion in the organic solvent and prevents aggregation of the particles forming a kinetically stable organosol in which were introduced the components of CIBA-GEIGY epoxide resin. An homogeneous hybrid composite material was obtained after heating at 60 °C for 24 hours.

Silica glass composites were prepared by polymerizing silicic acid or alkoxysilanes inside the aqueous sol of maghemite.[41,47,48] Hydrolysis and condensation of silanols take place *in situ* forming a gel and a transparent monolithic glass after drying at room temperature. These composites (Fig. 14) can contain up to 40 wt %

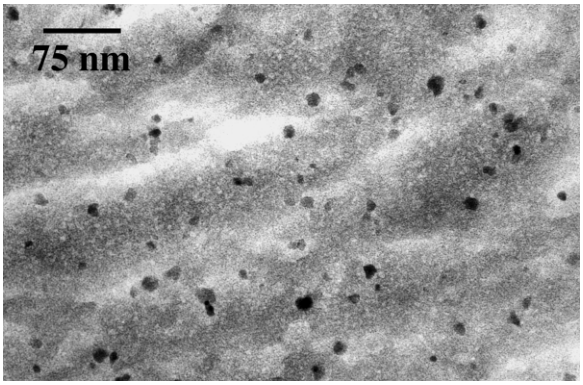

Fig. 14 TEM image of a thin slice of maghemite-silica composite (18 wt % Fe_2O_3).

Fe_2O_3. Infrared, near infrared and Mössbauer spectroscopies indicate no detectable Fe–O–Si bond in the samples formed from silicic acid or alkoxysilane. In fact, the dispersability of particles into the silica matrices results from solvation of silanol groups of the matrix by associated-water layers surrounding the particles, without other chemical surface interactions.

The silica matrix acts as an antisintering agent which stabilizes the maghemite particles against the thermal transformation into haematite. In composites with sufficiently low particle concentration, no transformation occurs as long as the matrix prevents the migration and coalescence of particles, that is, up to around 1000 °C, the temperature at which the glass softens or starts crystallizing.[49] Under oxygen flux, apart from texture effects, the two silica matrices behave in a similar way.[47] By heating at 1200 °C, the matrix partly crystallizes into cristobalite and the major iron oxide phase is the rarely observed polymorph ε–Fe_2O_3. The ε–Fe_2O_3 particles are globular in shape (Fig. 15) and correspond to a few

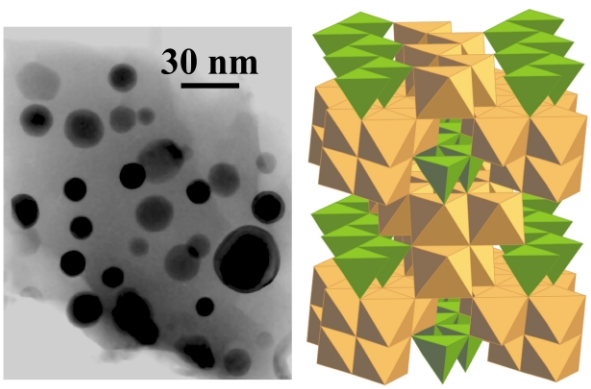

Fig. 15 TEM micrograph of a ε–Fe_2O_3-silica composite and crystal structure of ε–Fe_2O_3.

dozens of maghemite nanoparticles in volume. The crystal structure of ε–Fe_2O_3[49] is isotype with kappa alumina.[50,51] Mössbauer spectroscopic studies established that ε–Fe_2O_3 is a non-collinear ferrimagnet with a small net magnetization. It is probably piezoelectric.

At 1400 °C, the crystallization of the matrix is complete and iron oxide is transformed into haematite in form of crystals larger than those of ε–Fe_2O_3 by at least one order of magnitude. All observations indicate that ε–Fe_2O_3 forms as a result of the sintering of a limited number of γ–Fe_2O_3 nanoparticles. With powdered uncoated particles, the γ→α–Fe_2O_3 transformation starts below 300 °C and is generally complete at 400 to 500 °C.[51] In powders, the surface component in the total free energy of the transformation of iron oxide particles can be eliminated, so the free energy of the system can be minimized and the thermodynamically stable phase (haematite) is obtained. In the composites, when the diffusion of particles is limited, the decrease in surface area allows to lower the free energy of the system but the surface component remains important so that the minimum in free energy cannot be reached and a metastable phase forms. It could be possible that a careful control of the thermal treatments allows one to observe a series of phases intermediate between γ- and α–Fe_2O_3, like for alumina.

In the silica matrix formed from silane precursor, the Si–H bonds are surviving the hydrolysis, condensation and drying processes and so the matrix remains chemically reactive. By heating under argon flux, the cleavage of the Si–H bonds takes place from 450 to 1000 °C, allowing reduction of the maghemite particles into magnetite or metal with oxidation of the matrix into SiO_2. In concentrated samples, 80 w% γ–Fe_2O_3 corresponding to silica coated maghemite particles, the reduction of particles leads to magnetite because of too small a quantity of Si–H bonds in the matrix. The grains are however larger (D ≈ 25–30 nm) than the starting γ–Fe_2O_3 grains and stable up to at least 1400 °C. In diluted samples (18 w% γ–Fe_2O_3) the reduction leads to FeO and Fe_3O_4 at 500 °C and, at 1000 °C, to α–Fe grains *ca*. 30 nm in size.[47] From silica- Ni or Co hydroxides composites, this method allows to form cermets of ferromagnetic metal nanoparticles (Fe and also Ni and Co and alloys) protected against oxidation and suitable for instance for magnetic investigations.

4 Conclusions and perspectives

This overview emphasizes the high versatility of aqueous iron chemistry. It shows how to control the crystalline structure, the size and morphology of nanoparticles. It offers many possibilities for tailoring materials for a wide range of utilizations. The careful control of the size and degree of dispersion of the particles in composite materials could allow one to reveal unexpected phenomena.

The authors wish to thank their collaborators Ph. Belleville, Ph. Prené, L. Vayssières and J. Hernandez. J. M. Génin (Univ. Nancy) and P. Davidson (Univ. Paris-Sud Orsay) are greatfully acknowledged for fruitful collaborations. The authors also thank all physicist colleagues, especially M. Noguès (Univ. Versailles-Saint-Quentin) and D. Fiorani (CNR Roma) for their sustained interest in our magnetic materials.

Notes and references

1 R. M. Cornell and U. Schwertmann, *The iron oxides, structure, properties, reactions, occurrence and uses*, VCH Weinheim Germany Publishers (1996).
2 J. L. Dormann, D. Fiorani and E. Tronc, *Adv. Chem. Phys.*, 1997, **98**, 283.
3 W. Stumm and B. Sulzberger, *Geochim. et Cosmochim. Acta*, 1992, **56**, 3233.
4 S. Mann, J. Webb and R. J. P. Williams, *Biomineralization, Chemical and Biochemical Perspectives*. VCH Weinheim Germany Publishers (1989).
5 A. F. Wells, *Structural Inorganic Chemistry*, 5th ed., Oxford University Press, Oxford (1991).
6 E. Matijevic, *Pure Appl. Chem.*, 1988, **60**, 1479.
7 J.-P. Jolivet, *Metal Oxide Chemistry and Synthesis. From Solution to Solid State*, Wiley, Chichester (2000).
8 C. F. Baes and R. E Mesmer, *The Hydrolysis of Cations*, J. Wiley and Sons, New York, 1976.
9 S. J. Lippard, *Angew. Chem., Int. Ed. Engl.*, 1988, **27**, 344; K. L. Taft and S. J. Lippard, *J. Am. Chem. Soc*, 1990, **112**, 9629; W Schmitt *et al*,

Polyedron, 2001, **20**, 1687; L. F. Jones *et al.*, *Angew. Chem., Int. Ed. Engl.*, 2002, **41**, 4318.
10 H. Roussel, V. Briois, E. Elkaim, A. de Roy, J.-P. Besse and J.-P. Jolivet, *Chem. Mater.*, 2001, **13**, 329.
11 L. Spiccia and W. Marty, *Inorg. Chem.*, 1986, **25**, 266; L. Spiccia, W. Marty and R. Giovanoli, *Inorg. Chem.*, 1988, **27**, 2660.
12 L. Jambor and J. E. Dutrizac, *Chem. Rev.*, 1998, **98**, 2549; U. Schwertmann, J. Friedl and H. Stanjek, *J. Colloid Interface Sci.*, 1999, **209**, 215.
13 J. M. Combes, A. Manceau, G. Calas and J. Y. Bottero, *Geochim. Cosmochim. Acta*, 1989, **53**, 583.
14 P. Euzen, P. Raybaud, X. Krodikis, H. Toulhoat, J. L. Le Loaerer, J. P. Jolivet and C. Froidefond, *Handbook of Porous Solids*, Eds. F. Schüth, K. S. W. Sing and J. Weitkamp, Wiley-VCH, 1591 (2002).
15 R. L. Parfitt, S. J. van der Gast and C. W. Childs, *Clays Clay Miner*, 1992, **40**, 675; E. Doelsch, J. Rose, A. Masion, J. Y. Bottero, D. Nahon and P. M. Bertsch, *Langmuir*, 2000, **16**, 4726.
16 J. Rose, A. M. Flanck, A. Masion, J. Y. Bottero and F. Garcia, *Langmuir*, 1997, **12**, 6701; J. Rose, A. M. Flanck, A. Masion, J. Y. Bottero and P. Elmerich, *Langmuir*, 1997, **13**, 1827.
17 E. Pelegrin, PhD, Univ. Paris 7 (2000).
18 B. J. Lemaire, P. Davidson, J. Ferré, J. P. Jamet, P. Panine, I. Dozo and J. P. Jolivet, *Phys. Rev. Let.*, 2002, **88**, 125507.
19 J. Hernandez, C. Chanéac, , E. Tronc and J. P. Jolivet, forthcoming paper.
20 J. Y. Bottero, A. Manceau, F. Villieras and D. Tchoubar, *Langmuir*, 1994, **10**, 316; M. P. Morales, T. Gonzales-Carreno and C. J. Serna, *J. Mater. Res.*, 1992, **7**, 2538.
21 E. Matijevic and P. Scheiner, *J. Colloid Interface Sci.*, 1978, **63**, 509; T. Sugimoto, A. Muramatsu, K. Sakata and D. Shindo, *J. Colloid Interface Sci.*, 1993, **158**, 420; J. K. Bailey, C. J. Brinker and M. L. Mecartney, *J. Colloid Interface Sci.*, 1993, **157**, 1.
22 Ph. Refait, M. Abdelmoula and J.-M. R. Génin, *Corros. Sci.*, 1998, **40**, 1547; A. Géhin, C. Ruby, M. Abdelmoula, O. Benali, J. Ghanbaja, Ph. Refait and J.-M. R. Génin, *Sol. State Sci.*, 2002, **4**, 61.
23 C. Ruby, A. Géhin, M. Abdelmoula, J.-M. R. Génin and J.-P. Jolivet, *Sol. State Sci.*, 2003, **5**, 1055.
24 G. Ona-Nguema, M. Abdelmoula, F. Jorand, O. Benali, A. Géhin, J.-C. Block and J.-M. R. Génin, *Environ. Sci. Technol.*, 2002, **36**, 16.
25 F. Trolard, J.-M. R. Génin, M. Abdelmoula, G. Bourrié, B. Humbert and A. Herbillon, *Geochim. Cosmochim. Acta.*, 1997, **61**, 1107; G. Bourrié, F. Trolard, J.-M. R. Génin, A. Jaffrezic, V. Maître and M. Abdelmoula, *Geochim. Cosmochim. Acta.*, 1999, **63**, 3417.
26 J. P. Jolivet, P. Belleville, E. Tronc and J. Livage, *Clays Clay Miner.*, 1992, **40**, 531.
27 E. Tronc, P. Belleville, J. P. Jolivet and J. Livage, *Langmuir*, 1992, **8**, 313.
28 J. P. Jolivet, E. Tronc and C. Chanéac, *C. R. Chimie*, 2003, **5**, 659.
29 L. Vayssières, C. Chanéac, E. Tronc and J. P. Jolivet, *J. Colloid Interface Sci.*, 1998, **205**, 205; J. P. Jolivet, L. Vayssières, C. Chanéac and E. Tronc, *Mater. Res. Symp. Proc.*, 1997, **432**, 145.
30 J. P. Jolivet, C. Froidefond and C. Chanéac, in preparation.
31 J. P. Jolivet and E. Tronc, *J. Colloid Interface Sci.*, 1988, **125**, 688.
32 Tronc and J. P. Jolivet, *Adsorption Sci. Techn.*, 1984, **1**, 247; E. Tronc, J. P. Jolivet, J. Lefebvre and R. Massart, *J. Chem. Soc. Faraday Trans I*, 1984, **80**, 2619.
33 E. Tronc, J. P. Jolivet, P. Belleville and J. Livage, *Hyperf. Interact.*, 1989, **46**, 637.
34 P. Belleville, J. P. Jolivet, E. Tronc and J. Livage, *J. Colloid Interface Sci.*, 1992, **150**, 453.
35 J. P. Jolivet, E. Tronc, C. Barbé and J. Livage, *J. Colloid Interface Sci.*, 1990, **138**, 465.
36 J. P. Jolivet, R. Massart and J. M. Fruchart, *Nouv. J. Chim.*, 1983, **7**, 325.
37 P. Prené, E. Tronc, J. P. Jolivet, J. Livage, R. Cherkaoui, M. Noguès and J. L. Dormann, *IEEE Trans. Mag.*, 1993, **29**, 2658.
38 J. P. Jolivet, C. Chanéac, L. Vayssières and E. Tronc, *J. Phys. IV France*, 1997, **C1**, 573.
39 P. Fabre, C. Casagrande, M. Veyssié, V. Cabuil and R. Massart, *Phys. Rev. Lett.*, 1990, **64**, 539; J. C. Bacri, R. Perzinski, D. Salin, V. Cabuil and R. Massart, *J. Magn. Magn. Mater.*, 1990, **85**, 27; J. C. Dabadie, P. Fabre, M. Veyssié, V. Cabuil and R. Massart, *J. Phys. Condens. Matter*, 1990, 2; S. Lefebure, E. Dubois, V. Cabuil, S. Neveu and R. Massart, *Mater. Res.*, 1998, **13**, 2975; F. Cousin, E. Dubois and V. Cabuil, *Phys. Rev. E*, 2003, **68**, 21405.
40 H. Yokoi, K. Yagishita and Y. Nakanishi, *Bull. Chem. Soc. Jpn*, 1990, **63**, 746; C. W. Jung, *Magn. Reson. Imaging*, 1995, **13**, 675; J. Lee, T. Isobe and M. Senna, *J. Colloid Interface Sci.*, 1996, **177**, 490; E. Kroll, F. M. Winnik and R. F. Ziolo, *Chem. Mater.*, 1996, **8**, 1594; B. Z. Tang, Y. Geng, J. W. Y. Lam and B. Li, *Chem. Mater.*, 1999, **11**, 1581.
41 T. Gacoin, F. Chaput and J. P. Boilot, *J. Sol-Gel Sci. Techn.*, 1994, **2**, 679; A. P. Philipse, M. P. B. van Bruggen and C. Pathmama-Noharan, *Langmuir*, 1994, **10**, 92; G. Ennas, A. Musinu, G. Piccaluga, D. Zedda, D. Gatteschi, C. Sangregorio, J. L. Stanger, G. Concas and G. Spano, *Chem. Mater.*, 1998, **10**, 495; L. Casas, A. Roig, E. Rodriguez, E. Molins, J. Tejada and J. Sort, *J. Non-Cryst. Solds*, 2001, **285**, 37; M. F. Casula, A. Corrias and G. Pashina, *J. Non-Cryst. Solids*, 2001, **293–295**, 25; C. Cannas, M. F. Casula, G. Concas, A. Corrias, D. Gatteschi, A. Falqui, A. Musinu, C. Sangregorio and G. Spano, *J. Mater. Chem.*, 2001, **11**, 3180; G. Ennas, M. F. Casula, G. Piccaluga, S. Solinas, M. P. Morales and C. J. Serna, *J. Mater. Res*, 2002, **17**, 590; S. Mornet, F. Grasset, J. Portier and E. Duguet, *Eur. Cells Mater.*, 2002, **3**, 110.
42 E. Tronc, D. Fiorani, M. Noguès, A. M. Testa, F. Lucari, F. D'Orazio, J. M. Grenèche, W. Wernsdorfer, N. Galvez, C. Chanéac, D. Mailly and J. P. Jolivet, *J. Magn. Magn. Mater.*, 2003, **262**, 6.
43 P. Prené, E. Tronc, J. P. Jolivet, J. Livage, R. Cherkaoui, M. Noguès and J. L. Dormann, *Hyperf. Interact.*, 1994, **93**, 1409; E. Tronc, P. Prené, J. P. Jolivet, D. Fiorani, A. M. Testa, R. Cherkaoui, M. Noguès and J. L. Dormann, *Nanostructured Materials*, 1995, **6**, 945; D. Fiorani, A. M. Testa, E. Tronc, P. Prené, J. P. Jolivet, R. Cherkaoui, J. L. Dormann and M. Noguès, *J. Magn. Magn. Mater.*, 1995, **140–144**, 395; E. Tronc, P. Prené, J. P. Jolivet, F. d'Orazio, F. Lucari, D. Fiorani, M. Godinho, R. Cherkaoui, M. Noguès and J. L. Dormann, *Hyperf. Interact.*, 1995, **95**, 129; E. Tronc, A. Ezzir, R. Cherkaoui, C. Chanéac, M. Noguès, H. Kachkachi, D. Fiorani, A. M. Testa, J. M. Grenèche and J. P. Jolivet, *J. Magn. Magn. Mater.*, 2000, **221**, 63.
44 J. L. Dormann, F. d'Orazio, F. Lucari, E. Tronc, P. Prené, J. P. Jolivet, D. Fiorani, R. Cherkaoui and M. Noguès, *Phys. Rev. B*, 1996, **53**, 14291.
45 C. Chanéac, E. Tronc and J. P. Jolivet, *Mater. Res. Soc. Symp. Proc.*, 2000, **628**, CC641.
46 E. Tronc and J. P. Jolivet, *Hyperf. Interact.*, 1986, **28**, 525.
47 C. Chanéac, E. Tronc and J. P. Jolivet, *Nanostructured Materials*, 1995, **6**, 715.
48 C. Chanéac, E. Tronc and J. P. Jolivet, *J. Mater. Chem.*, 1996, 1905.
49 E. Tronc, C. Chanéac and J. P. Jolivet, *J. Solid State Chem.*, 1998, **139**, 93.
50 B. Ollivier, R. Retoux, P. Lacorre, D. Massiot and G. Férey, *J. Mater. Chem*, 1997, **7**, 1049.
51 E. Tronc, J. P. Jolivet and J. Livage, *Hyperf. Interact.*, 1990, **54**, 737.